41. PLOTS OF CROSS SECTIONS AND RELATED QUANTITIES

Jet Production in pp and $\overline{p}p$ Interactions

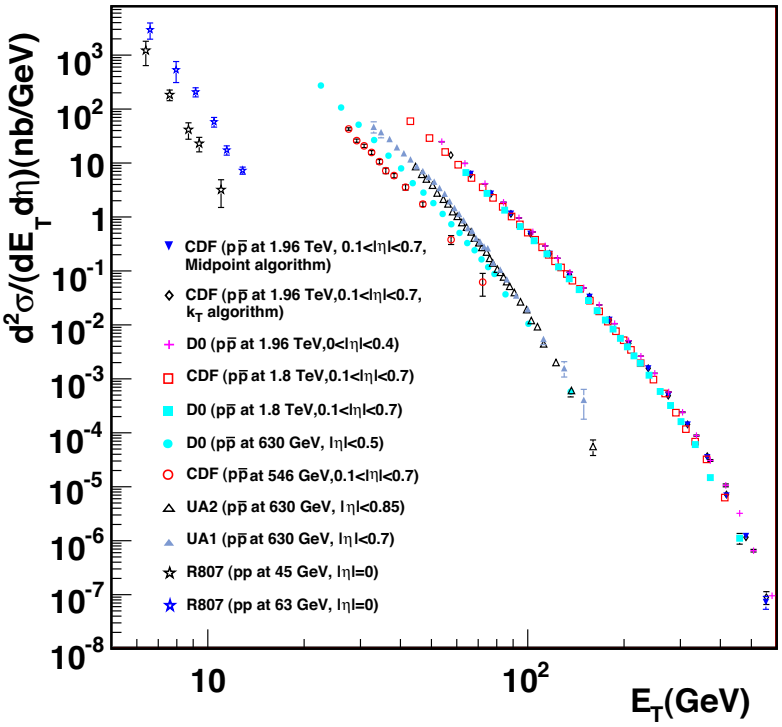

Figure 41.1: Inclusive differential jet cross sections plotted as a function of the jet tranverse energy. The CDF and D0 measurements use a cone algorithm of radius 0.7 for all results shown except for the CDF measurements at 1.96 TeV which also use k_T with a D parameter of 0.7 and midpoint algorithms. The cone/k_T results should be similar if $R_{cone} = D$. UA1 (UA2) uses a non-iterative cone algorithm with a radius of 1.0 (1.3). Recent NLO QCD predictions (such as CTEQ6M) provide a good description of the CDF and D0 jet cross sections, Rept. on Prog. in Phys. **70**, 89 (2007). Comparisons with the older cross sections are more difficult due to the nature of the jet algorithms used. **CDF**: Phys. Rev. **D75**, 092006 (2007), Phys. Rev. **D64**, 032001 (2001), Phys. Rev. Lett. **70**, 1376 (1993); **D0**: Phys. Rev. **D64**, 032003 (2001); **UA2**: Phys. Lett. **B257**, 232 (1991); **UA1**: Phys. Lett. **B172**, 461 (1986); **R807**: Phys. Lett. **B123**, 133 (1983). (Courtesy of J. Huston, Michigan State University, 2010.) See full-color version on color pages at end of book.

Direct γ Production in $\overline{p}p$ Interactions

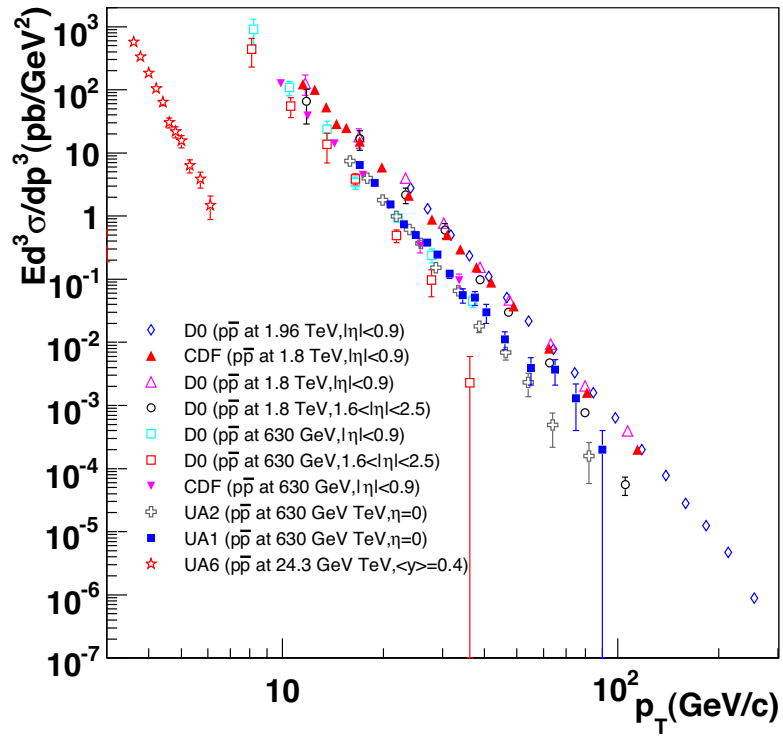

Figure 41.2: Isolated photon cross sections plotted as a function of the photon transverse momentum. The errors are either statistical only (CDF, D0 (1.96 TeV), UA1, UA2, UA6) or uncorrelated (D0 1.8 TeV, 630 GeV). The data are generally in good agreement with NLO QCD predictions, albeit with a tendency for the data to be above (below) the theory for lower (large) transverse momenta, Phys. Rev. **D59**, 074007 (1999). **D0**: Phys. Lett. **B639**, 151 (2006), Phys. Rev. Lett. **87**, 251805 (2001); **CDF**: Phys. Rev. **D65**, 112003 (2002); **UA6**: Phys. Lett. **B206**, 163 (1988); **UA1**: Phys. Lett. **B209**, 385 (1988); **UA2**: Phys. Lett. **B288**, 386 (1992). (Courtesy of J. Huston, Michigan State University, 2007.) See full-color version on color pages at end of book.

Differential Cross Section for W and Z Boson Production

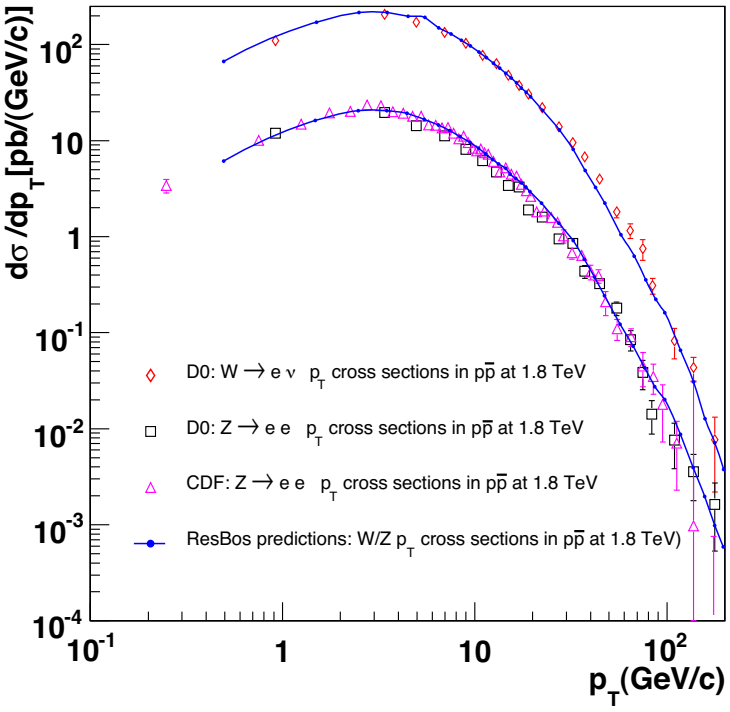

Figure 41.3: Differential cross sections for W and Z production shown as a function of the boson transverse momentum. The D0 results include only the statistical error while the CDF results include all errors except for the 3.9% integrated luminosity error. The results are in good agreement with theoretical predictions that include both the effects of NLO corrections and of q_T resummation, such as the ResBos (Phys. Rev. **D67**, 073016 (2003)) predictions indicated on the plot. **D0**: Phys. Lett. **B513**, 292 (2001), Phys. Rev. Lett. **84**, 2792 (2000). **CDF**: Phys. Rev. Lett. **84**, 845 (2000). (Courtesy of J. Huston, Michigan State University, 2007)

Pseudorapidity Distributions in $\overline{p}p$ Interactions

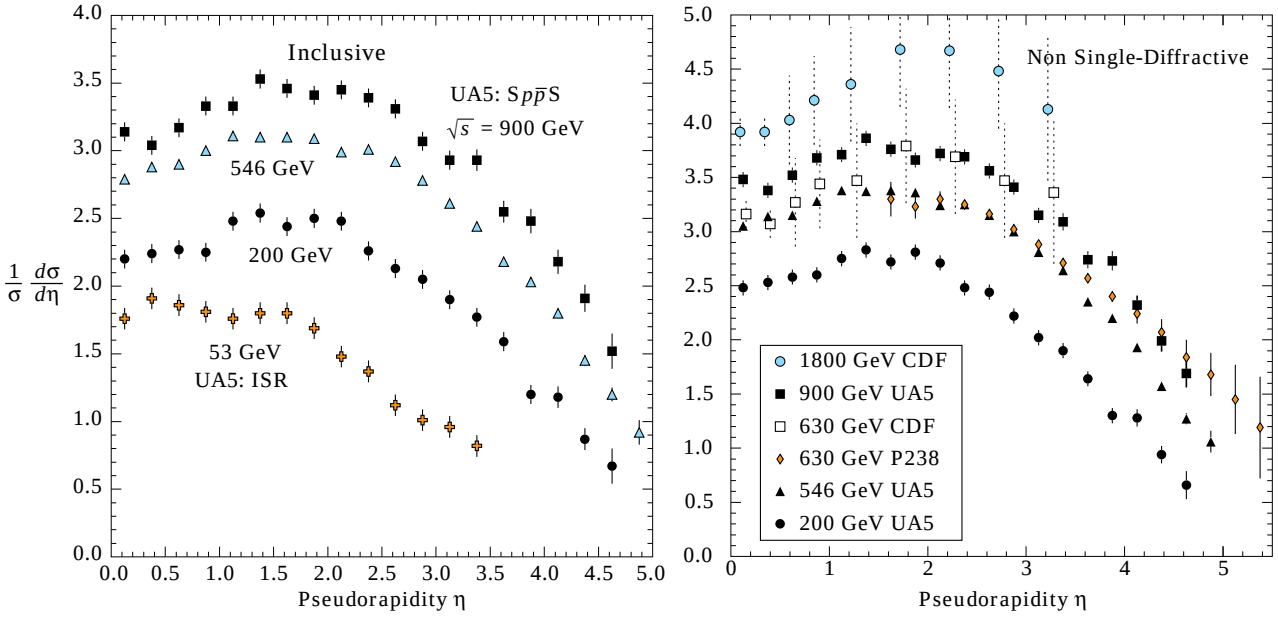

Figure 41.4: Charged particle pseudorapidity distributions in $p\overline{p}$ collisions for 53 GeV $\leq \sqrt{s} \leq$ 1800 GeV. UA5 data from the S$p\overline{p}$S are taken from G.J. Alner *et al.*, Z. Phys. **C33**, 1 (1986), and from the ISR from K. Alpgøard *et al.*, Phys. Lett. **112B**, 193 (1982). The UA5 data are shown for both the full inelastic cross section and with singly diffractive events excluded. Additional non single-diffractive measurements are available from CDF at the Tevatron, F. Abe *et al.*, Phys. Rev. **D41**, 2330 (1990) and Experiment P238 at the S$p\overline{p}$S, R. Harr *et al.*, Phys. Lett. **B401**, 176 (1997). (Courtesy of D.R. Ward, Cambridge Univ., 1999)

Average Hadron Multiplicities in Hadronic e^+e^- Annihilation Events

Table 41.1: Average hadron multiplicities per hadronic e^+e^- annihilation event at $\sqrt{s} \approx 10$, 29–35, 91, and 130–200 GeV. The rates given include decay products from resonances with $c\tau < 10$ cm, and include the corresponding anti-particle state. Correlations of the systematic uncertainties were considered for the calculation of the averages. (Updated May 2010 by O. Biebel, LMU, Munich)

Particle	$\sqrt{s} \approx 10$ GeV	$\sqrt{s} = 29$–35 GeV	$\sqrt{s} = 91$ GeV	$\sqrt{s} = 130$–200 GeV
Pseudoscalar mesons:				
π^+	6.6 ± 0.2	10.3 ± 0.4	17.02 ± 0.19	21.24 ± 0.39
π^0	3.2 ± 0.3	5.83 ± 0.28	9.42 ± 0.32	
K^+	0.90 ± 0.04	1.48 ± 0.09	2.228 ± 0.059	2.82 ± 0.19
K^0	0.91 ± 0.05	1.48 ± 0.07	2.049 ± 0.026	2.10 ± 0.12
η	0.20 ± 0.04	0.61 ± 0.07	1.049 ± 0.080	
$\eta'(958)$	0.03 ± 0.01	0.26 ± 0.10	0.152 ± 0.020	
D^+	$0.194 \pm 0.019^{(a)}$	0.17 ± 0.03	0.175 ± 0.016	
D^0	$0.446 \pm 0.032^{(a)}$	0.45 ± 0.07	0.454 ± 0.030	
D_s^+	$0.063 \pm 0.014^{(a)}$	$0.45 \pm 0.20^{(b)}$	0.131 ± 0.021	
$B^{(c)}$	—	—	$0.165 \pm 0.026^{(d)}$	
B^+	—	—	$0.178 \pm 0.006^{(d)}$	
B_s^0	—	—	$0.057 \pm 0.013^{(d)}$	
Scalar mesons:				
$f_0(980)$	0.024 ± 0.006	$0.05 \pm 0.02^{(e)}$	0.146 ± 0.012	
$a_0(980)^\pm$	—	—	$0.27 \pm 0.11^{(f)}$	
Vector mesons:				
$\rho(770)^0$	0.35 ± 0.04	0.81 ± 0.08	1.231 ± 0.098	
$\rho(770)^\pm$	—	—	$2.40 \pm 0.43^{(f)}$	
$\omega(782)$	0.30 ± 0.08	—	1.016 ± 0.065	
$K^*(892)^+$	0.27 ± 0.03	0.64 ± 0.05	0.715 ± 0.059	
$K^*(892)^0$	0.29 ± 0.03	0.56 ± 0.06	0.738 ± 0.024	
$\phi(1020)$	0.044 ± 0.003	0.085 ± 0.011	0.0963 ± 0.0032	
$D^*(2010)^+$	$0.177 \pm 0.022^{(a)}$	0.43 ± 0.07	$0.1937 \pm 0.0057^{(g)}$	
$D^*(2007)^0$	$0.168 \pm 0.019^{(a)}$	0.27 ± 0.11	—	
$D_s^*(2112)^+$	$0.048 \pm 0.014^{(a)}$	—	$0.101 \pm 0.048^{(h)}$	
$B^{*\ (i)}$	—	—	0.288 ± 0.026	
$J/\psi(1S)$	$0.00050 \pm 0.00005^{(a)}$	—	$0.0052 \pm 0.0004^{(j)}$	
$\psi(2S)$	—	—	$0.0023 \pm 0.0004^{(j)}$	
$\Upsilon(1S)$	—	—	$0.00014 \pm 0.00007^{(j)}$	
Pseudovector mesons:				
$f_1(1285)$	—	—	0.165 ± 0.051	
$f_1(1420)$	—	—	0.056 ± 0.012	
$\chi_{c1}(3510)$	—	—	$0.0041 \pm 0.0011^{(j)}$	
Tensor mesons:				
$f_2(1270)$	0.09 ± 0.02	0.14 ± 0.04	0.166 ± 0.020	
$f_2'(1525)$	—	—	0.012 ± 0.006	
$K_2^*(1430)^+$	—	0.09 ± 0.03	—	
$K_2^*(1430)^0$	—	0.12 ± 0.06	0.084 ± 0.022	
$B^{**\ (k)}$	—	—	0.118 ± 0.024	
$D_{s1}^\pm$	—	—	$0.0052 \pm 0.0011^{(\ell)}$	
$D_{s2}^{*\pm}$	—	—	$0.0083 \pm 0.0031^{(\ell)}$	
Baryons:				
p	0.253 ± 0.016	0.640 ± 0.050	1.050 ± 0.032	1.41 ± 0.18
Λ	0.080 ± 0.007	0.205 ± 0.010	0.3915 ± 0.0065	0.39 ± 0.03
Σ^0	0.023 ± 0.008	—	0.076 ± 0.011	
Σ^-	—	—	0.081 ± 0.010	
Σ^+	—	—	0.107 ± 0.011	
$\Sigma^\pm$	—	—	0.174 ± 0.009	
Ξ^-	0.0059 ± 0.0007	0.0176 ± 0.0027	0.0258 ± 0.0010	
$\Delta(1232)^{++}$	0.040 ± 0.010	—	0.085 ± 0.014	
$\Sigma(1385)^-$	0.006 ± 0.002	0.017 ± 0.004	0.0240 ± 0.0017	
$\Sigma(1385)^+$	0.005 ± 0.001	0.017 ± 0.004	0.0239 ± 0.0015	
$\Sigma(1385)^\pm$	0.0106 ± 0.0020	0.033 ± 0.008	0.0462 ± 0.0028	
$\Xi(1530)^0$	0.0015 ± 0.0006	—	0.0068 ± 0.0006	
Ω^-	0.0007 ± 0.0004	0.014 ± 0.007	0.0016 ± 0.0003	
Λ_c^+	$0.074 \pm 0.031^{(m)}$	0.110 ± 0.050	0.078 ± 0.017	
Λ_b^0	—	—	0.031 ± 0.016	
$\Sigma_c^{++}, \Sigma_c^0$	0.014 ± 0.007	—	—	
$\Lambda(1520)$	0.008 ± 0.002	—	0.0222 ± 0.0027	

Notes for Table 41.1:

(*a*) $\sigma_{\rm had} = 3.33 \pm 0.05 \pm 0.21$ nb (**CLEO**: Phys. Rev. **D29**, 1254 (1984)) has been used in converting the measured cross sections to average hadron multiplicities.

(*b*) B($D_s \to \eta\pi,\ \eta'\pi$) was used (RPP 1994).

(*c*) Comprises both charged and neutral B meson states.

(*d*) The Standard Model B($Z \to b\overline{b}$) = 0.217 was used.

(*e*) $x_p = p/p_{\rm beam} > 0.1$ only.

(*f*) Both charge states.

(*g*) B($D^*(2010)^+ \to D^0\pi^+$) × B($D^0 \to K^-\pi^+$) has been used (RPP 2000).

(*h*) B($D_s^* \to D_S^+\gamma$), B($D_s^+ \to \phi\pi^+$), B($\phi \to K^+K^-$) have been used (RPP 1998).

(*i*) Any charge state (*i.e.*, B_d^*, B_u^*, or B_s^*).

(*j*) B($Z \to$ hadrons) = 0.699 was used (RPP 1994).

(*k*) Any charge state (*i.e.*, B_d^{**}, B_u^{**}, or B_s^{**}).

(ℓ) Assumes B($D_{s1}^+ \to D^{*+}K^0 + D^{*0}K+$) = 100% and B($D_{s2}^+ \to D^0K^+$) = 45%.

(*m*) The value was derived from the cross section of $\Lambda_c^+ \to p\pi K$ using (*a*) and assuming the branching fraction to be (5.0 ± 1.3)% (RPP 2004).

References for Table 41.1:

RPP 1992: Phys. Rev. **D45** (1992) and references therein.

RPP 1994: Phys. Rev. **D50**, 1173 (1994) and references therein.

RPP 1996: Phys. Rev. **D54**, 1 (1996) and references therein.

RPP 1998: Eur. Phys. J. **C3**, 1 (1998) and references therein.

RPP 2000: Eur. Phys. J. **C15**, 1 (2000) and references therein.

RPP 2002: Phys. Rev. **D66**, 010001 (2002) and references therein.

RPP 2004: Phys. Lett. **B592**, 1 (2004) and references therein.

RPP 2006: J. Phys. **G33**, 1 (2006) and references therein.

RPP 2008: Phys. Lett. **B667**, 1 (2008) and references therein.

R. Marshall, Rept. on Prog. in Phys. **52**, 1329 (1989). A. De Angelis, J. Phys. **G19**, 1233 (1993) and references therein.

ALEPH: D. Buskulic *et al.*: Phys. Lett. **B295**, 396 (1992); Z. Phys. **C64**, 361 (1994); **C69**, 15 (1996); **C69**, 379 (1996); **C73**, 409 (1997); and R. Barate *et al.*: Z. Phys. **C74**, 451 (1997); Phys. Reports **294**, 1 (1998); Eur. Phys. J. **C5**, 205 (1998); **C16**, 597 (2000); **C16**, 613 (2000); and A. Heister *et al.*: Phys. Lett. **B526**, 34 (2002); **B528**, 19 (2002).

ARGUS: H. Albrecht *et al.*: Phys. Lett. **230B**, 169 (1989); Z. Phys. **C44**, 547 (1989); **C46**, 15 (1990); **C54**, 1 (1992); **C58**, 199 (1993); **C61**, 1 (1994); Phys. Rep. **276**, 223 (1996).

BaBar: B. Aubert *et al.*: Phys. Rev. Lett. **87**, 162002 (2001); Phys. Rev. **D65**, 091104 (2002).

Belle: K. Abe *et al.*, Phys. Rev. Lett. **88**, 052001 (2002); and R. Seuster *et al.*, Phys. Rev. **D73**, 032002 (2006).

CELLO: H.J. Behrend *et al.*: Z. Phys. **C46**, 397 (1990); **C47**, 1 (1990).

CLEO: D. Bortoletto *et al.*, Phys. Rev. **D37**, 1719 (1988); erratum *ibid.* **D39**, 1471 (1989); and M. Artuso *et al.*, Phys. Rev. **D70**, 112001 (2004).

Crystal Ball: Ch. Bieler *et al.*, Z. Phys. **C49**, 225 (1991).

DELPHI: P. Abreu *et al.*: Z. Phys. **C57**, 181 (1993); **C59**, 533 (1993); **C61**, 407 (1994); **C65**, 587 (1995); **C67**, 543 (1995); **C68**, 353 (1995); **C73**, 61 (1996); Nucl. Phys. **B444**, 3 (1995); Phys. Lett. **B341**, 109 (1994); **B345**, 598 (1995); **B361**, 207 (1995); **B372**, 172 (1996); **B379**, 309 (1996); **B416**, 233 (1998); **B449**, 364 (1999); **B475**, 429 (2000); Eur. Phys. J. **C6**, 19 (1999); **C5**, 585 (1998); **C18**, 203 (2000); and J. Abdallah *et al.*, Phys. Lett. **B569**, 129 (2003); Phys. Lett. **B576**, 29 (2003); Eur. Phys. J. **C44**, 299 (2005); and W. Adam *et al.*: Z. Phys. **C69**, 561 (1996); **C70**, 371 (1996).

HRS: S. Abachi *et al.*, Phys. Rev. Lett. **57**, 1990 (1986); and M. Derrick *et al.*, Phys. Rev. **D35**, 2639 (1987).

L3: M. Acciarri *et al.*: Phys. Lett. **B328**, 223 (1994); **B345**, 589 (1995); **B371**, 126 (1996); **B371**, 137 (1996); **B393**, 465 (1997); **B404**, 390 (1997); **B407**, 351 (1997); **B407**, 389 (1997), erratum *ibid.* **B427**, 409 (1998); **B453**, 94 (1999); **B479**, 79 (2000).

MARK II: H. Schellman *et al.*, Phys. Rev. **D31**, 3013 (1985); and G. Wormser *et al.*, Phys. Rev. Lett. **61**, 1057 (1988).

JADE: W. Bartel *et al.*, Z. Phys. **C20**, 187 (1983); and D.D. Pietzl *et al.*, Z. Phys. **C46**, 1 (1990).

OPAL: R. Akers *et al.*: Z. Phys. **C63**, 181 (1994); **C66**, 555 (1995); **C67**, 389 (1995); **C68**, 1 (1995); and G. Alexander *et al.*: Phys. Lett. **B358**, 162 (1995); Z. Phys. **C70**, 197 (1996); **C72**, 1 (1996); **C72**, 191 (1996); **C73**, 569 (1997); **C73**, 587 (1997); Phys. Lett. **B370**, 185 (1996); and
K. Ackerstaff *et al.*: Z. Phys. **C75**, 192 (1997); Phys. Lett. **B412**, 210 (1997); Eur. Phys. J. **C1**, 439 (1998); **C4**, 19 (1998); **C5**, 1 (1998); **C5**, 411 (1998); and G. Abbiendi *et al.*: Eur. Phys. J. **C16**, 185 (2000); **C17**, 373 (2000).

PLUTO: Ch. Berger *et al.*, Phys. Lett. **104B**, 79 (1981).

SLD: K. Abe, Phys. Rev. **D59**, 052001 (1999); Phys. Rev. **D69**, 072003 (2004).

TASSO: H. Aihara *et al.*, Z. Phys. **C27**, 27 (1985).

TPC: H. Aihara *et al.*, Phys. Rev. Lett. **53**, 2378 (1984).

Average e^+e^-, pp, and $\overline{p}p$ Multiplicity

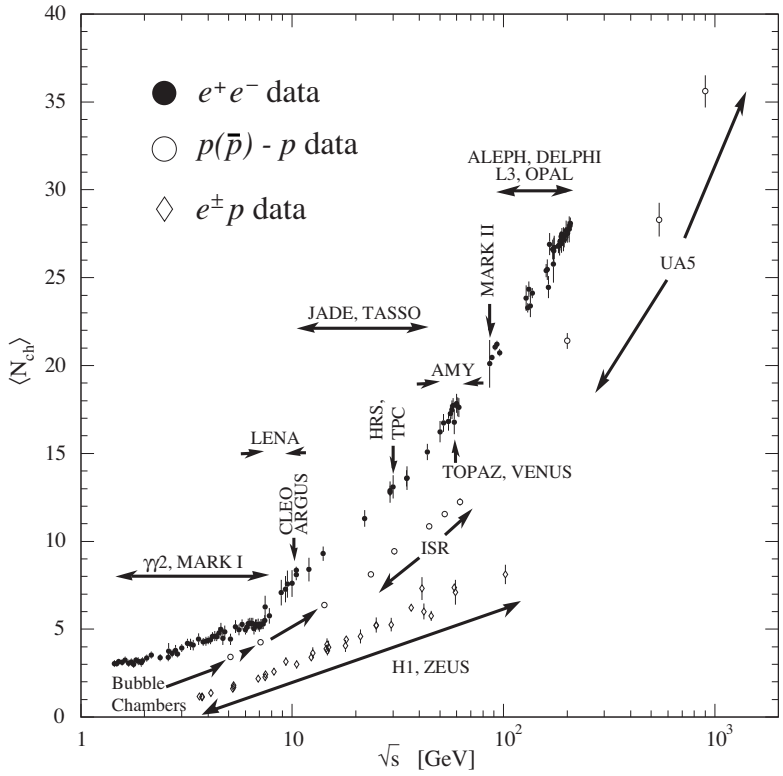

Figure 41.5: Average multiplicity as a function of $\sqrt{s}$ for e^+e^- and $p\overline{p}$ annihilations, and pp and ep collisions. The indicated errors are statistical and systematic errors added in quadrature, except when no systematic errors are given. Files of the data shown in this figure are given in `http://pdg.lbl.gov/current/avg-multiplicity/`.

—

***e*$^+$*e*$^-$**: Most e^+e^- measurements include contributions from K^0_S and Λ decays. The $\gamma\gamma 2$ and MARK I measurements contain a systematic 5% error. Points at identical energies have been spread horizontally for clarity:

ALEPH: D. Buskulic *et al.*, Z. Phys. **C69**, 15 (1995); and Z. Phys. **C73**, 409 (1997);
A. Heister *et al.*, Eur. Phys. J. **C35**, 457 (2004).

ARGUS: H. Albrecht *et al.*, Z. Phys. **C54**, 13 (1992).

DELPHI: P. Abreu *et al.*, Eur. Phys. J. **C6**, 19 (1999); Phys. Lett. **B372**, 172 (1996); Phys. Lett. **B416**, 233 (1998); and Eur. Phys. J. **C18**, 203 (2000).

L3: M. Acciarri *et al.*, Phys. Lett. **B371**, 137 (1996); Phys. Lett. **B404**, 390 (1997); and Phys. Lett. **B444**, 569 (1998);
P. Achard *et al.*, Phys. Reports **339**, 71 (2004).

OPAL: G. Abbiendi *et al.*, Eur. Phys. J. **C16**, 185 (2000); and Eur. Phys. J. **C37**, 25 (2004);
K. Ackerstaff *et al.*, Z. Phys. **C75**, 193 (1997);
P.D. Acton *et al.*, Z. Phys. **C53**, 539 (1992) and references therein;
R. Akers *et al.*, Z. Phys. **C68**, 203 (1995).

TOPAZ: K. Nakabayashi *et al.*, Phys. Lett. **B413**, 447 (1997).

VENUS: K. Okabe *et al.*, Phys. Lett. **B423**, 407 (1998).

—

e*$^\pm$*p: Multiplicities have been measured in the current fragmentation region of the Breit frame:

H1: C. Adloff *et al.*, Nucl. Phys. **B504**, 3 (1997); F.D. Aaron *et al.*, Phys. Lett. **B654**, 148 (2007).

ZEUS: J. Breitweg *et al.*, Eur. Phys. J. **C11**, 251 (1999);
S. Chekanov *et al.*, Phys. Lett. **B510**, 36 (2001).

—

***p*$^{(-)}$**: The errors of the $p^{(-)}$ measurements are the quadratically added statistical and systematic errors, except for the bubble chamber measurements for which only statistical errors are given in the references. The values measured by UA5 exclude single diffractive dissociation:

bubble chamber: J. Benecke *et al.*, Nucl. Phys. **B76**, 29 (1976); W.M. Morse *et al.*, Phys. Rev. **D15**, 66 (1977).

ISR: A. Breakstone *et al.*, Phys. Rev. **D30**, 528 (1984).

UA5: G.J. Alner *et al.*, Phys. Lett. **167B**, 476 (1986);
R.E. Ansorge *et al.*, Z. Phys. **C43**, 357 (1989).

(Courtesy of O. Biebel, LMU, Munich, 2010)

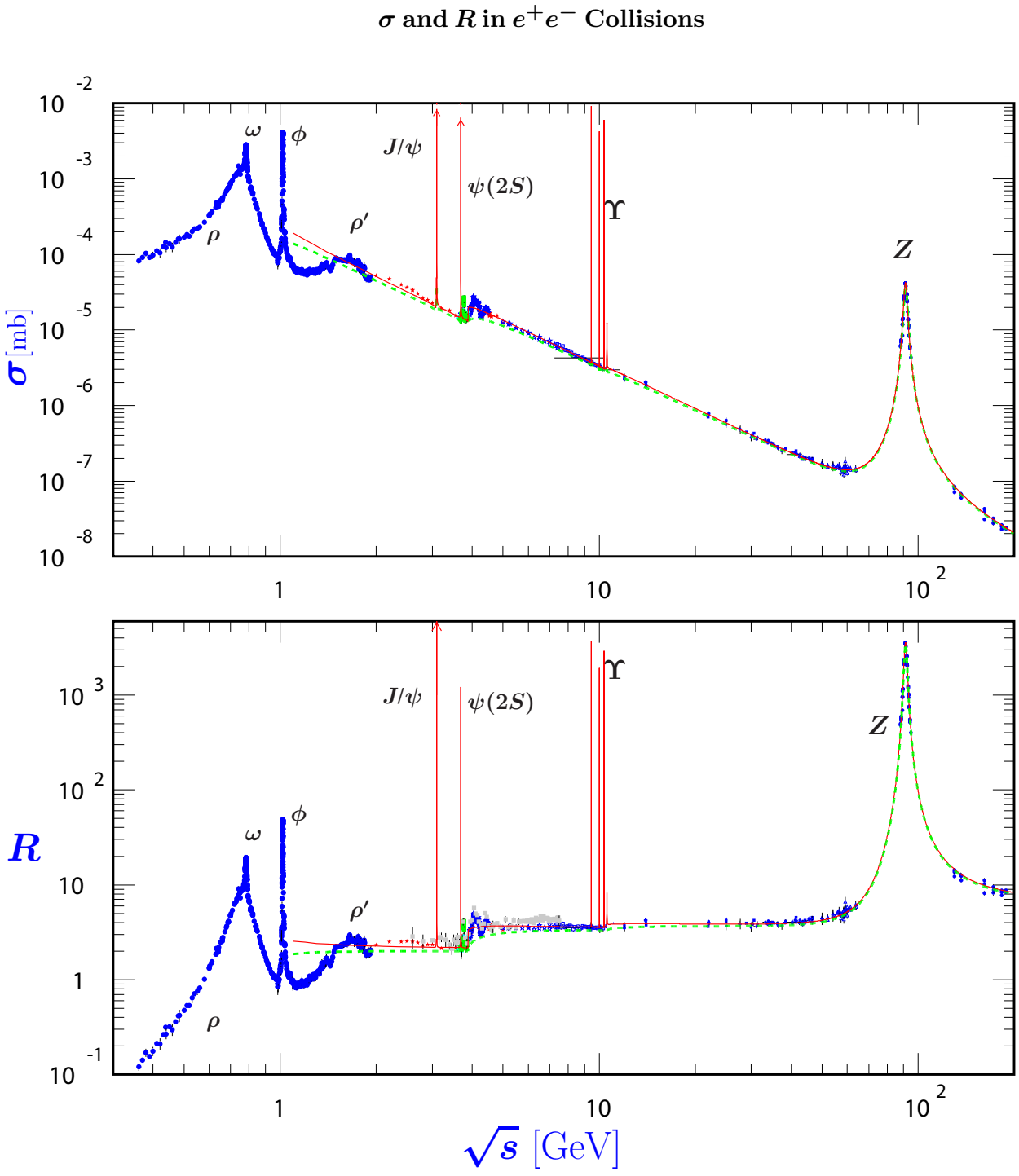

Figure 41.6: World data on the total cross section of $e^+e^- \to hadrons$ and the ratio $R(s) = \sigma(e^+e^- \to hadrons, s)/\sigma(e^+e^- \to \mu^+\mu^-, s)$. $\sigma(e^+e^- \to hadrons, s)$ is the experimental cross section corrected for initial state radiation and electron-positron vertex loops, $\sigma(e^+e^- \to \mu^+\mu^-, s) = 4\pi\alpha^2(s)/3s$. Data errors are total below 2 GeV and statistical above 2 GeV. The curves are an educative guide: the broken one (green) is a naive quark-parton model prediction, and the solid one (red) is 3-loop pQCD prediction (see "Quantum Chromodynamics" section of this *Review*, Eq. (9.7) or, for more details, K. G. Chetyrkin *et al.*, Nucl. Phys. **B586**, 56 (2000) (Erratum *ibid.* **B634**, 413 (2002)). Breit-Wigner parameterizations of J/ψ, $\psi(2S)$, and $\Upsilon(nS), n = 1, 2, 3, 4$ are also shown. The full list of references to the original data and the details of the R ratio extraction from them can be found in `[arXiv:hep-ph/0312114]`. Corresponding computer-readable data files are available at `http://pdg.lbl.gov/current/xsect/`. (Courtesy of the COMPAS (Protvino) and HEPDATA (Durham) Groups, May 2010.) See full-color version on color pages at end of book.

R in Light-Flavor, Charm, and Beauty Threshold Regions

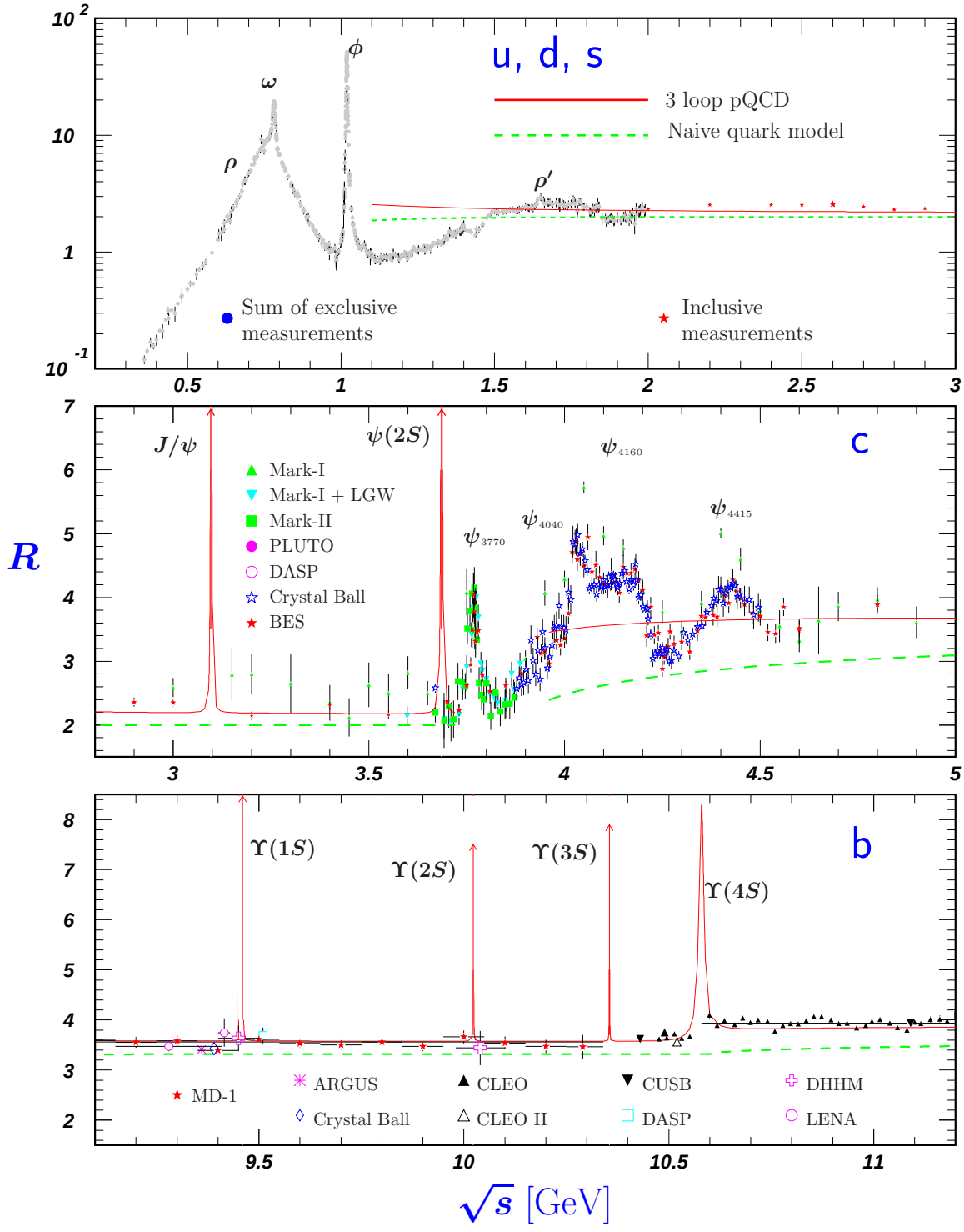

Figure 41.7: R in the light-flavor, charm, and beauty threshold regions. Data errors are total below 2 GeV and statistical above 2 GeV. The curves are the same as in Fig. 41.6. **Note:** CLEO data above $\Upsilon(4S)$ were not fully corrected for radiative effects, and we retain them on the plot only for illustrative purposes with a normalization factor of 0.8. The full list of references to the original data and the details of the R ratio extraction from them can be found in `[arXiv:hep-ph/0312114]`. The computer-readable data are available at `http://pdg.lbl.gov/current/xsect/`. (Courtesy of the COMPAS (Protvino) and HEPDATA (Durham) Groups, May 2010.) See full-color version on color pages at end of book.

Annihilation Cross Section Near M_Z

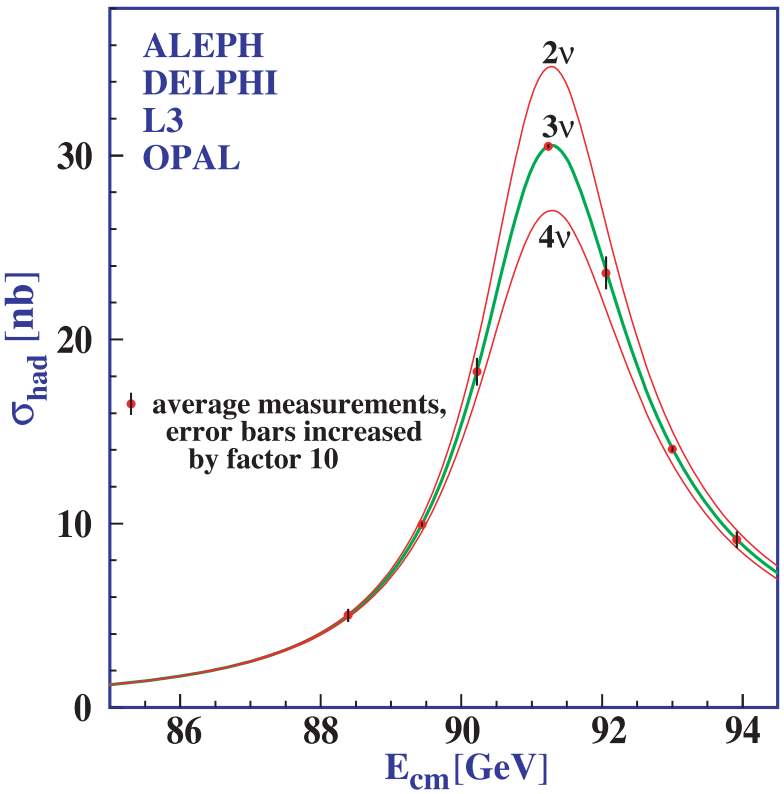

Figure 41.8: Combined data from the ALEPH, DELPHI, L3, and OPAL Collaborations for the cross section in e^+e^- annihilation into hadronic final states as a function of the center-of-mass energy near the Z pole. The curves show the predictions of the Standard Model with two, three, and four species of light neutrinos. The asymmetry of the curve is produced by initial-state radiation. Note that the error bars have been increased by a factor ten for display purposes. References:

ALEPH: R. Barate *et al.*, Eur. Phys. J. **C14**, 1 (2000).
DELPHI: P. Abreu *et al.*, Eur. Phys. J. **C16**, 371 (2000).
L3: M. Acciarri *et al.*, Eur. Phys. J. **C16**, 1 (2000).
OPAL: G. Abbiendi *et al.*, Eur. Phys. J. **C19**, 587 (2001).
Combination: The ALEPH, DELPHI, L3, OPAL, SLD Collaborations, the LEP Electroweak Working Group, and the SLD Electroweak and Heavy Flavor Groups, Phys. Rept. **427**, 257 (2006) [arXiv:hep-ex/0509008].

(Courtesy of M. Grünewald and the LEP Electroweak Working Group, 2007)

Muon Neutrino and Anti-Neutrino Charged-Current Total Cross Section

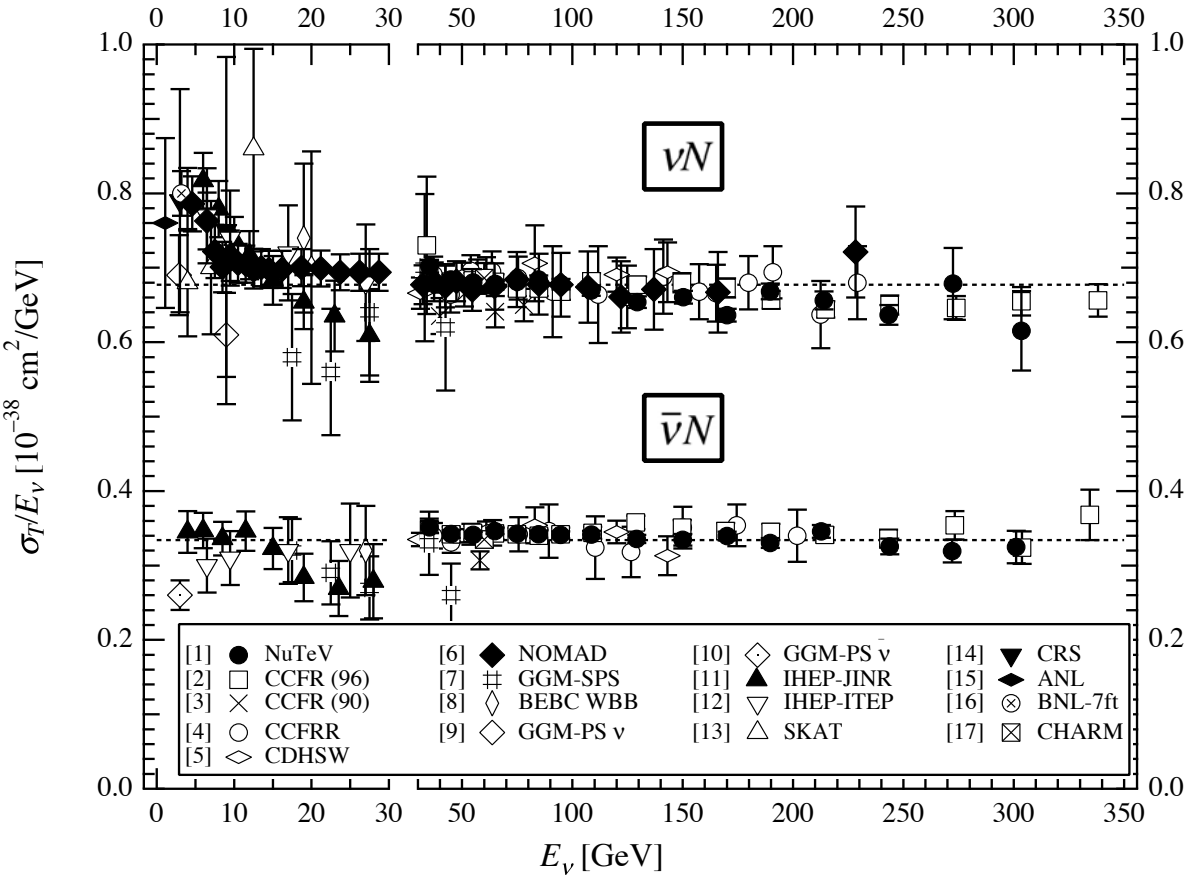

Figure 41.9: σ_T/E_ν for the muon neutrino and anti-neutrino charged-current total cross section as a function of neutrino energy. The error bars include both statistical and systematic errors. The straight lines are the isoscalar-corrected total cross-section values averaged over 30-200 *GeV* as measured by the experiments in Refs. [3–5]: $\sigma^{\nu\,Iso}/E_\nu = (0.677 \pm 0.014) \times 10^{-38}\mathrm{cm}^2/\mathrm{GeV}$; $\sigma^{\bar{\nu}\,Iso}/E_{\bar{\nu}} = (0.334 \pm 0.008) \times 10^{-38}\mathrm{cm}^2/\mathrm{GeV}$. The average ratio of the anti-neutrino to neutrino cross section in the energy range 30-200 GeV is $\sigma^{\bar{\nu}\,Iso}/\sigma^{\nu\,Iso} = 0.504 \pm 0.003$ as measured by Refs. [1–5]. Note the change in the energy scale at 30 GeV. (Courtesy W. Seligman and M.H. Shaevitz, Columbia University, 2010)

[1] M. Tzanov *et al.*, Phys. Rev. **D74**, 012008 (2006);
[2] W. Seligman, Ph.D. Thesis, Nevis Report 292 (1996);
[3] P.S. Auchincloss *et al.*, Z. Phys. **C48**, 411 (1990);
[4] D.B. MacFarlane *et al.*, Z. Phys. **C26**, 1 (1984);
[5] P. Berge *et al.*, Z. Phys. **C35**, 443 (1987);
[6] Q. Wu *et al.*, Phys. Lett. **B660**, 19 (2008);
[7] J. Morfin *et al.*, Phys. Lett. **B104**, 235 (1981);
[8] D.C. Colley *et al.*, Z. Phys. **C2**, 187 (1979);
[9] S. Campolillo *et al.*, Phys. Lett. **B84**, 281 (1979);
[10] O. Erriquez *et al.*, Phys. Lett. **B80**, 309 (1979);
[11] V.B. Anikeev *et al.*, Z. Phys. **C70**, 39 (1996);
[12] A.S. Vovenko *et al.*, Sov. J. Nucl. Phys. **30**, 527 (1979);
[13] D.S. Baranov *et al.*, Phys. Lett. **B81**, 255 (1979);
[14] C. Baltay *et al.*, Phys. Rev. Lett. **44**, 916 (1980);
[15] S.J. Barish *et al.*, Phys. Lett. **B66**, 291 (1977);
[16] N.J. Baker *et al.*, Phys. Rev. **D25**, 617 (1982);
[17] J.V. Allaby *et al.*, Z. Phys. **C38**, 403 (1988).

Table 41.2: Total hadronic cross section. Analytic S-matrix and Regge theory suggest a variety of parameterizations of total cross sections at high energies with different areas of applicability and fits quality.

A ranking procedure, based on measures of different aspects of the quality of the fits to the current evaluated experimental database, allows one to single out the following parameterization of highest rank[1]

$$\sigma^{ab} = Z^{ab} + B\log^2(s/s_0) + Y_1^{ab}(s_1/s)^{\eta_1} - Y_2^{ab}(s_1/s)^{\eta_2}\ , \qquad \sigma^{\overline{a}b} = Z^{ab} + B\log^2(s/s_0) + Y_1^{ab}(s_1/s)^{\eta_1} + Y_2^{ab}(s_1/s)^{\eta_2}\ ,$$

where Z^{ab}, B, Y_i^{ab} are in mb, and s, s_1, and s_0 are in GeV^2. The scales s_0, s_1, the rate of universal rise of the cross sections B, and exponents η_1 and η_2 are independent of the colliding particles. The scale s_1 is fixed at 1 GeV^2. Terms $Z^{ab} + B\log^2(s/s_0)$ represent the pomerons. The exponents η_1 and η_2 represent lower-lying C-even and C-odd exchanges, respectively. Requiring $\eta_1 = \eta_2$ results in somewhat poorer fits. In addition to total cross sections σ, the measured ratios of the real-to-imaginary parts of the forward scattering amplitudes $\rho = \mathrm{Re}(T)/\mathrm{Im}(T)$ were included in the fits by using s to u crossing symmetry. Global fits were made to the 2005-updated data for $\overline{p}(p)p$, $\Sigma^- p$, $\pi^\pm p$, $K^\pm p$, γp, and $\gamma\gamma$ collisions.

Exact factorization hypothesis in the form $(Z^{\gamma p}, B^{\gamma p}) = \delta \cdot (Z^{pp}, B)$, $(Z^{\gamma\gamma}, B^{\gamma\gamma}) = \delta^2 \cdot (Z^{pp}, B)$ was used to extend the universal rise of the total hadronic cross sections to the $\gamma p \to hadrons$ and $\gamma\gamma \to hadrons$ collisions. This resulted in reducing the number of adjusted parameters from 21 used for the 2002 edition to 19, and in the higher quality rank of the parameterization. The asymptotic parameters thus obtained were then fixed and used as inputs to a fit to a larger data sample that included cross sections on deuterons (d) and neutrons (n). All fits included data above $\sqrt{s_{\min}} = 5$ GeV.

Fits to $\overline{p}(p)\,p$, $\Sigma^- p$, $\pi^\pm p$, $K^\pm p$, γp, $\gamma\gamma$			Beam/	Fits to groups				χ^2/dof
Z	Y_1	Y_2	Target	Z	Y_1	Y_2	B	by groups
35.45(48)	42.53(1.35)	33.34(1.04)	$\overline{p}(p)/p$	35.45(48)	42.53(23)	33.34(33)	0.308(10)	
			$\overline{p}(p)n$	35.80(16)	40.15(1.59)	30.00(96)	0.308(10)	1.029
35.20(1.46)	−199(102)	−264(126)	Σ^-/p	35.20(1.41)	−199(86)	−264(112)	0.308(10)	0.565
20.86(40)	19.24(1.22)	6.03(19)	$\pi^\pm/p$	20.86(3)	19.24(18)	6.03(9)	0.308(10)	0.955
17.91(36)	7.1(1.5)	13.45(40)	$K^\pm/p$	17.91(3)	7.14(25)	13.45(13)	0.308(10)	
			$K^\pm/n$	17.87(6)	5.17(50)	7.23(28)	0.308(10)	0.669
0.0317(6)			γ/p		0.0320(40)		0.308(10)	
−0.61(62)E−3			γ/γ		−0.58(61)E−3		0.308(10)	0.766
$\chi^2/dof = 0.971$,	$B = 0.308(10)$ mb,		$\overline{p}(p)/d$	64.35(38)	130(3)	85.5(1.3)	0.537(31)	1.432
$\eta_1 = 0.458(17)$,	$\eta_2 = 0.545(7)$		$\pi^\pm/d$	38.62(21)	59.62(1.53)	1.60(41)	0.461(14)	0.735
$\delta = 0.00308(2)$,	$\sqrt{s_0} = 5.38(50)$ GeV		$K^\pm/d$	33.41(20)	23.66(1.45)	28.70(37)	0.449(14)	0.814

The fitted functions are shown in the following figures, along with one-standard-deviation error bands. When the reduced χ^2 is greater than one, a scale factor has been included to evaluate the parameter values, and to draw the error bands. Where appropriate, statistical and systematic errors were combined quadratically in constructing weights for all fits. On the plots, only statistical error bars are shown. Vertical arrows indicate lower limits on the p_{lab} or E_{cm} range used in the fits.

One can find the details of the global fits and ranking procedure, in the paper [1]. Database is practically the same as for the 2004 edition (it was slightly changed in the low energy regions not used in the fits).

Recently, the statement in [1] that the models with $\log^2(s/s_0)$ asymptotic terms work much better than the models with $\log(s/s_0)$ or $(s/s_0)^\epsilon$ terms was confirmed in [2] and [3], based on matching traditional asymptotic parameterizations with low energy data in different ways. Both these references, however, questioned the statement in [1] on the universality of the coefficient of the $\log^2(s/s_0)$ term for all processes with nucleon and gamma targets. The two references give different predictions at superhigh energies: $\sigma^{as}_{\pi N} > \sigma^{as}_{NN}$ [2] and $\sigma^{as}_{\pi N} \sim 2/3\sigma^{as}_{NN}$ [3]. A broader universality of σ^{as}_{tot} has been recently advocated in [4] for hadron-nucleus collisions. It should be noted that asymptotic rate universality in hadron-deuteron collisions has not been established at available energies (see Table).

Computer-readable data files are available at `http://pdg.lbl.gov/current/xsect/`. (Courtesy of the COMPAS group, IHEP, Protvino, August 2005)

On-line "Predictor" to calculate σ and ρ for any energy from five high rank models is also available at `http://nuclth02.phys.ulg.ac.be/compete/predictor/`.

References:

1. J.R. Cudell *et al.* (COMPETE Collab.), Phys. Rev. **D65**, 074024 (2002).
2. K. Igi and M. Ishida, Phys. Rev. **D66**, 034023 (2002), Phys. Lett. **B622**, 286 (2005).
3. M. M. Block and F. Halzen, Phys. Rev. **D70**, 091901 (2004), Phys. Rev. **D72**, 036006 (2005).
4. L. Frankfurt, M. Strikman, and M. Zhalov, Phys. Lett. **B616**, 59 (2005).

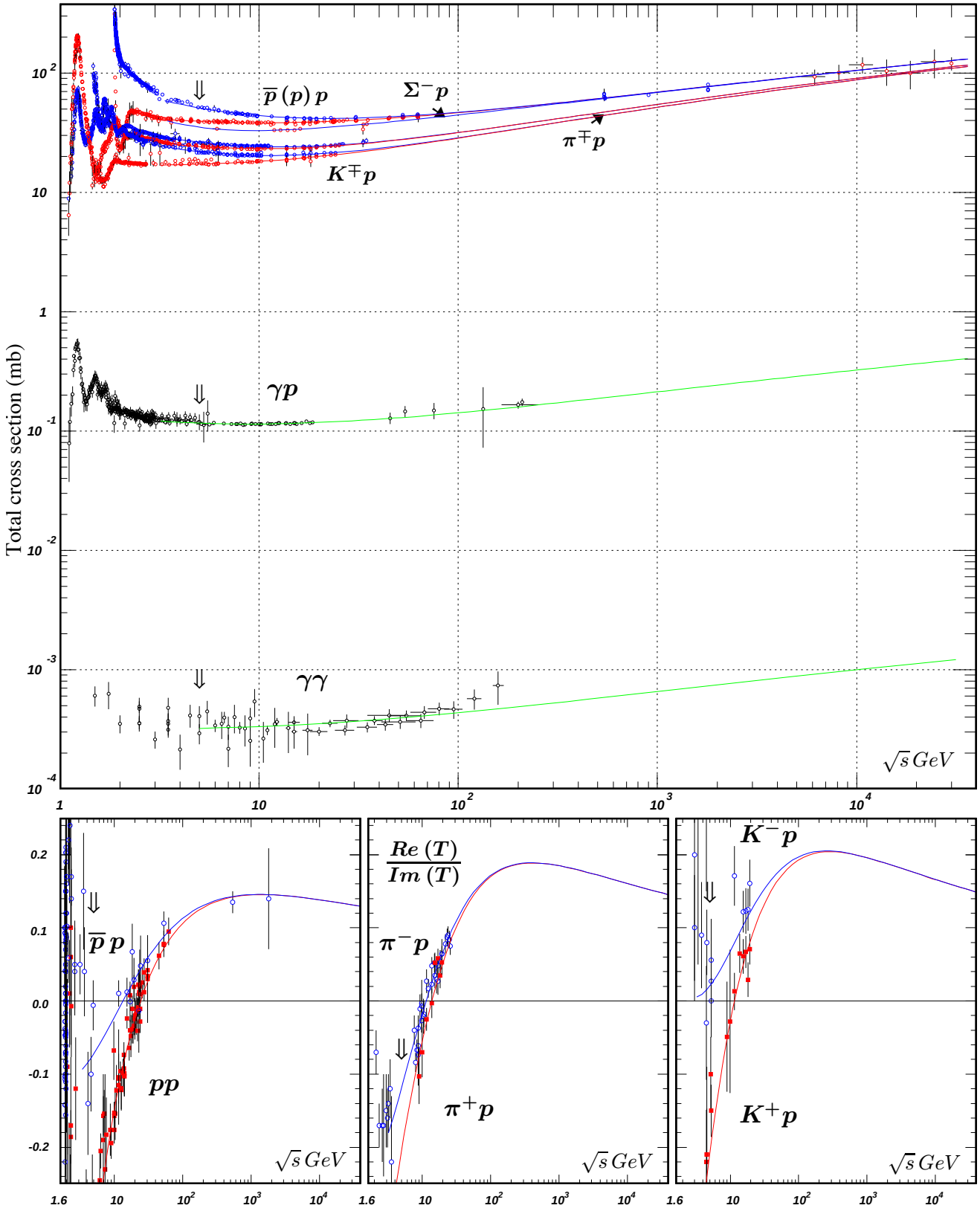

Figure 41.10: Summary of hadronic, γp, and $\gamma\gamma$ total cross sections, and ratio of the real to imaginary parts of the forward hadronic amplitudes. Corresponding computer-readable data files may be found at `http://pdg.lbl.gov/current/xsect/`. (Courtesy of the COMPAS group, IHEP, Protvino, August 2005.) See full-color version on color pages at end of book.

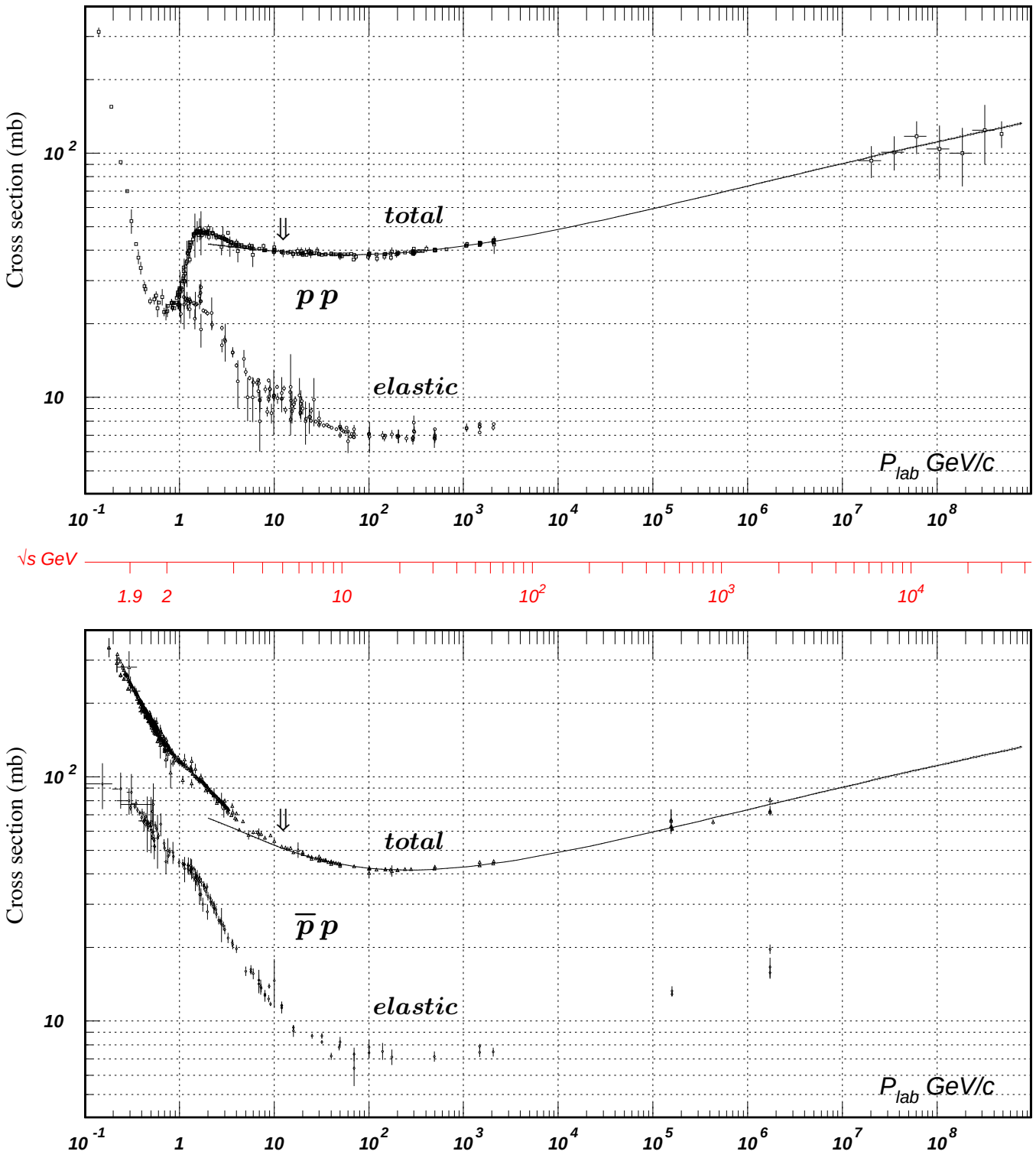

Figure 41.11: Total and elastic cross sections for pp and $\overline{p}p$ collisions as a function of laboratory beam momentum and total center-of-mass energy. Corresponding computer-readable data files may be found at `http://pdg.lbl.gov/current/xsect/`. (Courtesy of the COMPAS group, IHEP, Protvino, August 2005)

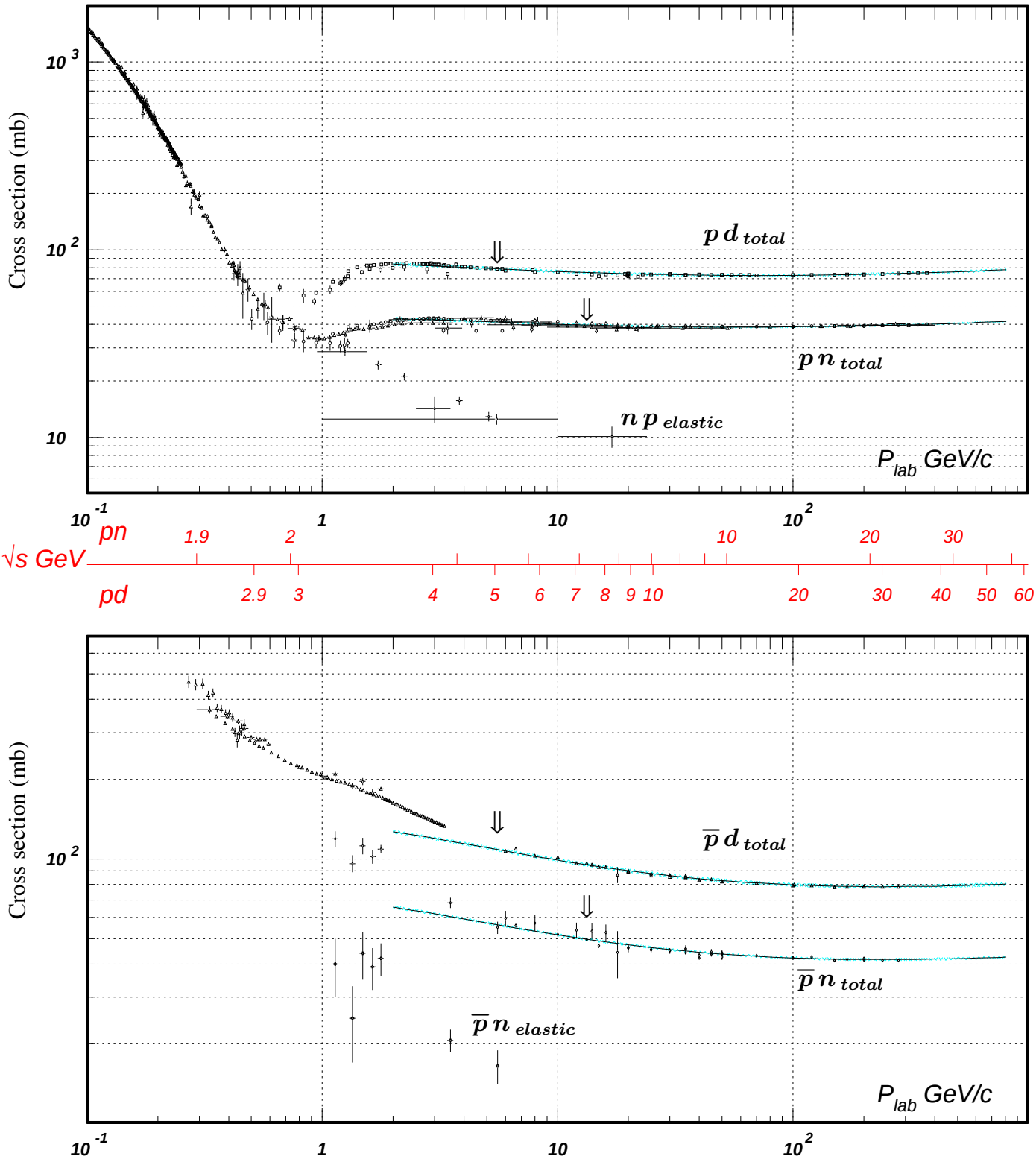

Figure 41.12: Total and elastic cross sections for pd (total only), np, $\overline{p}d$ (total only), and $\overline{p}n$ collisions as a function of laboratory beam momentum and total center-of-mass energy. Corresponding computer-readable data files may be found at `http://pdg.lbl.gov/current/xsect/`. (Courtesy of the COMPAS Group, IHEP, Protvino, August 2005)

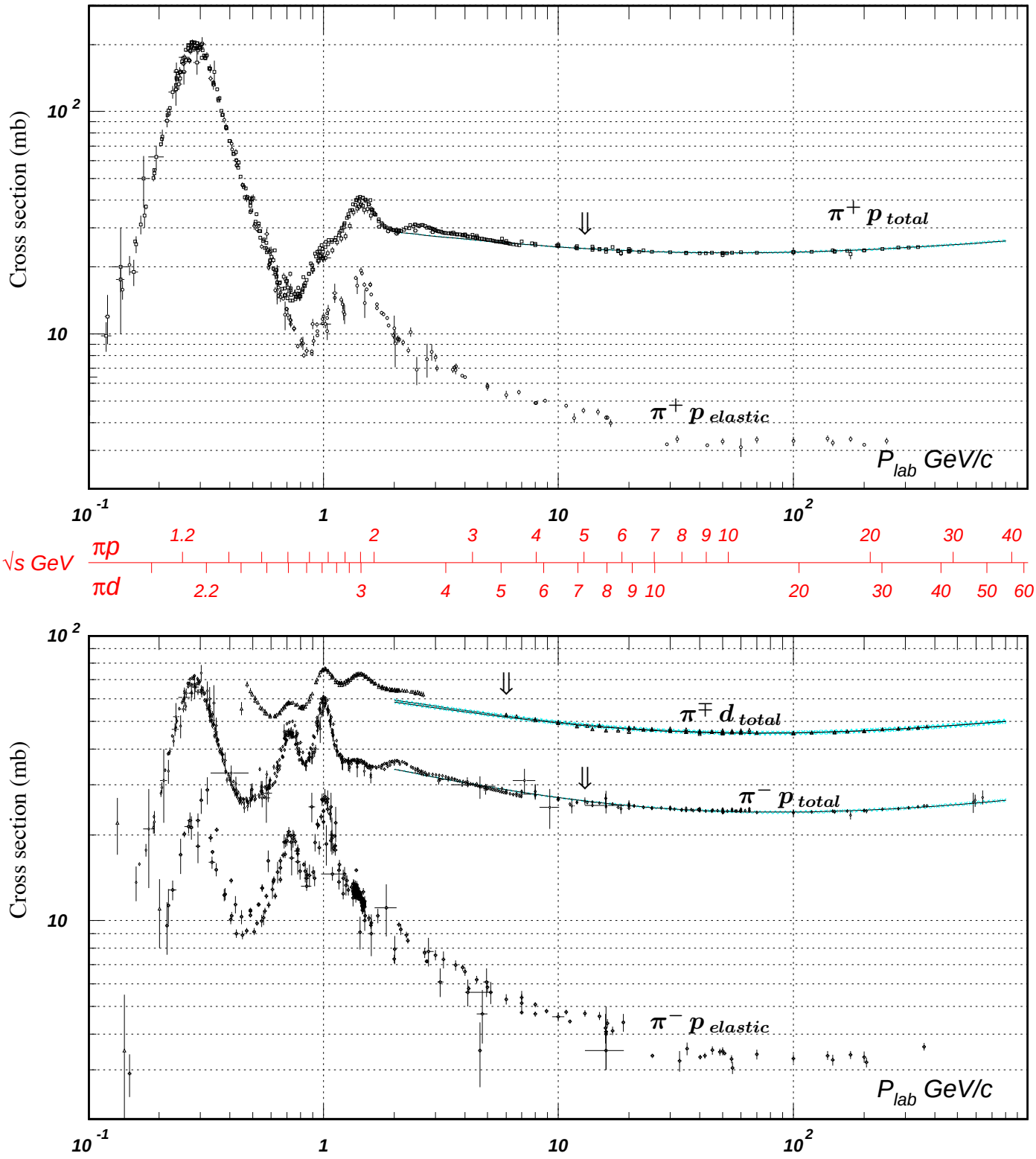

Figure 41.13: Total and elastic cross sections for $\pi^{\pm}p$ and $\pi^{\pm}d$ (total only) collisions as a function of laboratory beam momentum and total center-of-mass energy. Corresponding computer-readable data files may be found at `http://pdg.lbl.gov/current/xsect/`. (Courtesy of the COMPAS Group, IHEP, Protvino, August 2005)

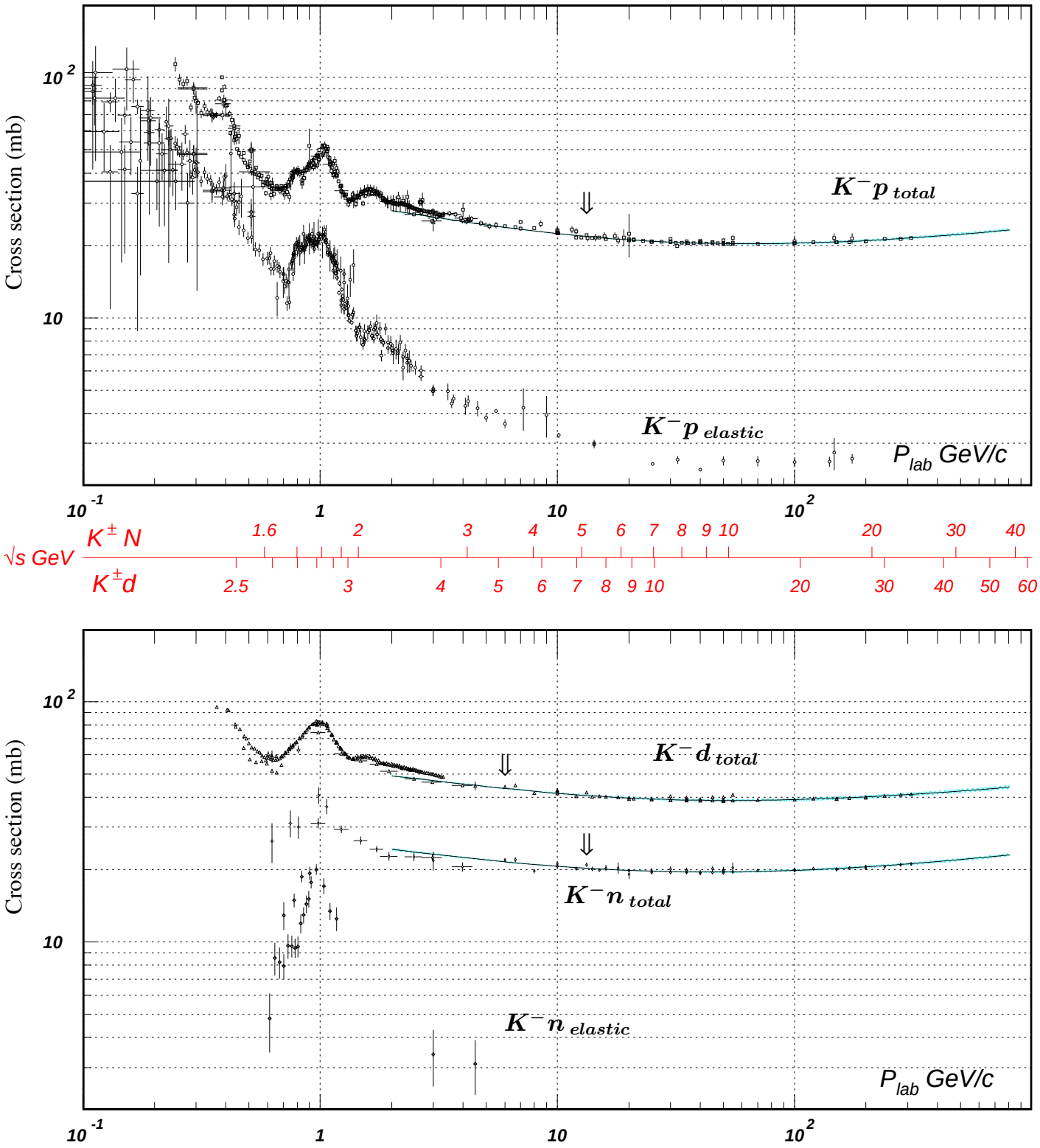

Figure 41.14: Total and elastic cross sections for $K^- p$ and $K^- d$ (total only), and $K^- n$ collisions as a function of laboratory beam momentum and total center-of-mass energy. Corresponding computer-readable data files may be found at `http://pdg.lbl.gov/current/xsect/`. (Courtesy of the COMPAS Group, IHEP, Protvino, August 2005)

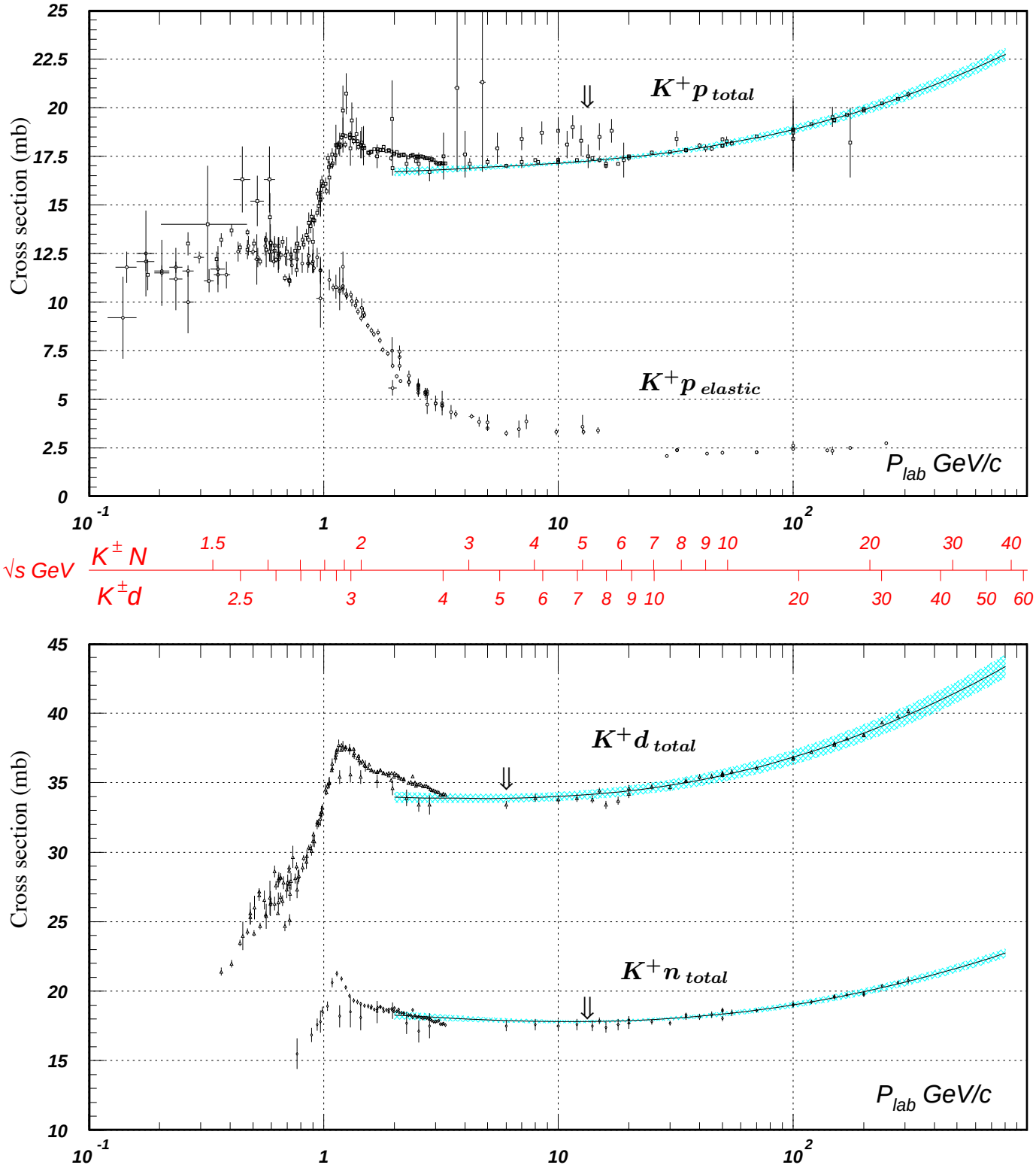

Figure 41.15: Total and elastic cross sections for K^+p and total cross sections for K^+d and K^+n collisions as a function of laboratory beam momentum and total center-of-mass energy. Corresponding computer-readable data files may be found at `http://pdg.lbl.gov/current/xsect/`. (Courtesy of the COMPAS Group, IHEP, Protvino, August 2005)

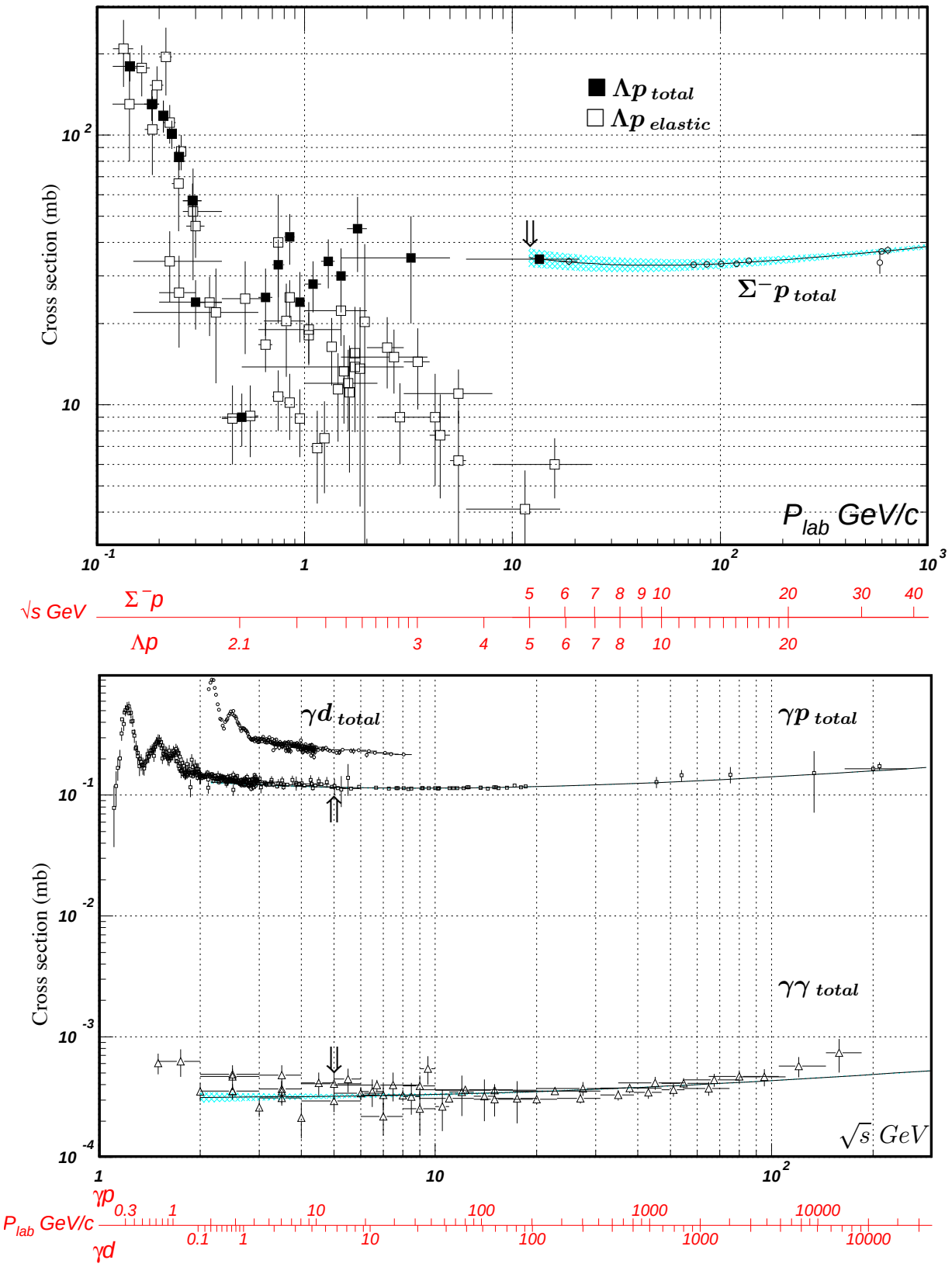

Figure 41.16: Total and elastic cross sections for Λp, total cross section for $\Sigma^- p$, and total hadronic cross sections for γd, γp, and $\gamma\gamma$ collisions as a function of laboratory beam momentum and the total center-of-mass energy. Corresponding computer-readable data files may be found at `http://pdg.lbl.gov/current/xsect/`. (Courtesy of the COMPAS group, IHEP, Protvino, August 2005)